LETTER Communicated by Walter Senn

Synaptic and Temporal Ensemble Interpretation of Spike-Timing-Dependent Plasticity

Peter A. Appleby
paa02r@ecs.soton.ac.uk
Terry Elliott
te@ecs.soton.ac.uk
Department of Electronics and Computer Science, University of Southampton, Highfield, Southampton SO17 1BJ, U.K.

We postulate that a simple, three-state synaptic switch governs changes in synaptic strength at individual synapses. Under this switch rule, we show that a variety of experimental results on timing-dependent plasticity can emerge from temporal and spatial averaging over multiple synapses and multiple spike pairings. In particular, we show that a critical window for the interaction of pre- and postsynaptic spikes emerges as an ensemble property of the collective system, with individual synapses exhibiting only a minimal form of spike coincidence detection. In addition, we show that a Bienenstock-Cooper-Munro–like, rate-based plasticity rule emerges directly from such a model. This demonstrates that two apparently separate forms of neuronal plasticity can emerge from a much simpler rule governing the plasticity of individual synapses.

1 Introduction

In addition to standard, rate-based long term potentiation (rLTP) (Bliss & Lømo, 1973; Gustafsson, Wigström, Abraham, & Huang, 1987; Dudek & Bear, 1992), a second form of activity-dependent synaptic plasticity governed by the exact timing of pre- and postsynaptic stimulation has recently been shown to operate in the nervous system (for review, see Roberts & Bell, 2002). This form of plasticity is widespread, appearing in the hippocampus (Bi & Poo, 1998; Debanne, Gähwiler, & Thompson, 1998), visual pathway (Zhang, Tao, Holt, Harris, & Poo, 1998), neocortex (Markram, Lübke, Frotscher, & Sakmann, 1997; Egger, Feldmeyer, & Sakmann, 1999; Feldman, 2000; Froemke & Dan, 2002), and even the electric fish electrosensory lobe (Bell, Han, Sugawara, & Grant, 1997). A critical window for the interaction of the pre- and postsynaptic events is seen, with separations greater than around 50 ms failing to evoke any change. Within this window, the degree of modification is a function of the spike timing, and the phenomenon has become known as timing-dependent LTP (tLTP). In most cases, presynaptic spiking followed by postsynaptic spiking (positively correlated spiking)

leads to potentiation, while reversing the order of spiking (negatively correlated spiking) leads to depression (but see Bell et al., 1997). Several variations have been observed in vivo and in vitro, with marked differences in the width of the critical window (Debanne et al., 1998), degree of potentiation and depression (Egger et al., 1999), or polarity of change (Bell et al., 1997).

In theoretical studies, the potentiation and depression phases of the tLTP modification curve have mainly been approximated by two exponential functions with different amplitudes, polarities, and decay constants, and then applied directly as a rule to determine changes in synaptic strength. This carries with it the implicit assumptions that the tLTP curve is valid at each individual synapse and that all the synapses making up the overall connection evolve similarly. In conjunction with certain constraints, this method can give rise to stable distributions of synaptic efficacies with competitive dynamics either emerging directly or introduced by synaptic scaling (Song, Miller, & Abbott, 2000; van Rossum, Bi, & Turrigiano, 2000; Izhikevich & Desai, 2003). If the tLTP rule really is implemented at individual synapses, then each synapse must possess machinery capable of resolving pre- and postsynaptic spike timing with millisecond accuracy. Although mechanisms capable of operating as coincidence detectors may be present at the synapse, it is not clear that they can resolve spike timing with the level of accuracy needed by these models. Other models of tLTP have been built using a more biophysical approach, employing the idea that the NMDA receptor may serve as the required molecular coincidence detector (Castellani, Quinlan, Cooper, & Shouval, 2001; Karmarkar & Buonomano, 2002; Shouval, Bear, & Cooper, 2002). However, these models can be rather sensitive to the choice of parameters and sometimes predict a rarely observed, extra depressive phase at large spike timings (but see Nishiyama, Hong, Mikoshiba, Poo, & Kato, 2000). Experimental results based on spike triplet and quadruplet interactions (Froemke & Dan, 2002) instead of spike pair interactions demonstrate, moreover, that such interactions evoke changes in overall synaptic strength that are inconsistent with a simple, additive model employing the tLTP rule on the embedded spike pair sequences. Modifying the simple tLTP model to include constraints on spike interactions such as spike suppression does, however, allow the triplet and quadruplet results to be accommodated (Froemke & Dan, 2002).

These various approaches to tLTP, although widely adopted, should be viewed with some caution. The experimental evidence for tLTP involves measuring the change in the overall connection strength between pre- and postsynaptic cells after many spike pairings. However, this overall change could arise, for example, from some simpler plasticity rule operating at individual synapses, and only when the change in the overall strength is viewed as a spatial and temporal average over these many individual changes might the overall change appear to follow a tLTP-like rule. That is, the tLTP curve may be an emergent, ensemble property of synapses but

not actually instantiated at any individual synapse. Here we postulate such a rule governing individual synaptic changes and show that the observed tLTP curve can indeed emerge as a temporal and spatial average over multiple synapses and multiple spike pairings. The rule is robust under highly variable spike timings and eliminates the need for synapses to exhibit millisecond resolution coincidence detection. An explanation of spike triplet interactions emerges as a natural consequence of its structure, with no need to introduce additional constraints. We also show that a Bienenstock-Cooper-Munro (BCM)–like (Bienenstock, Cooper, & Munro, 1982), rate-based plasticity rule emerges directly from such a model.

2 Formulation of Model

We now construct an activity-dependent synaptic plasticity rule that governs changes at individual synapses in response to pre- and postsynaptic spiking. We propose that a positively correlated spike pair will potentiate a given synapse by a fixed amount A_+, subject only to the requirement that the postsynaptic spike occurs within a finite time window relative to the presynaptic spike. Outside this time window, the postsynaptic spike does not evoke any change in synaptic strength. The duration of this time window is not fixed, but is taken to be a stochastic quantity governed by some probability distribution. This simple modification rule could be embodied by some biological, synaptic switch mechanism. The arrival of a presynaptic spike activates some process that elevates the synapse into a different functional state. The arrival of a postsynaptic spike while this process is still active, and the synapse is still in the elevated state, induces potentiation of the synapse by a fixed amount A_+. The postsynaptic spike is also taken to deactivate the process. In the absence of postsynaptic firing, the process will naturally deactivate in a stochastic, random manner, and subsequent postsynaptic spiking will not evoke a change in synaptic strength unless preceded by further presynaptic spiking.

We label the resting state of the synapse as the *OFF* state. The elevation of the synapse into a different functional state, due to the arrival of a presynaptic spike, is represented by a transition to a different state that we label the *POT* state. While in the *POT* state, additional presynaptic spiking has no further effect. If, on the other hand, a postsynaptic spike occurs while the switch is in the *POT* state, then the switch is immediately returned to the *OFF* state via the transition $POT \to OFF$. This transition is defined to induce an associated potentiation of synaptic strength of A_+. In the absence of further spiking, the switch will move from the *POT* state back to the *OFF* state in a stochastic manner, governed by some probability distribution. We refer to transitions triggered by pre- or postsynaptic spiking as *active transitions*, while those that occur stochastically are referred to as *passive transitions*. This abstracted rule is represented in Figure 1A, with semicircles representing active transitions and wavy lines representing passive transitions.

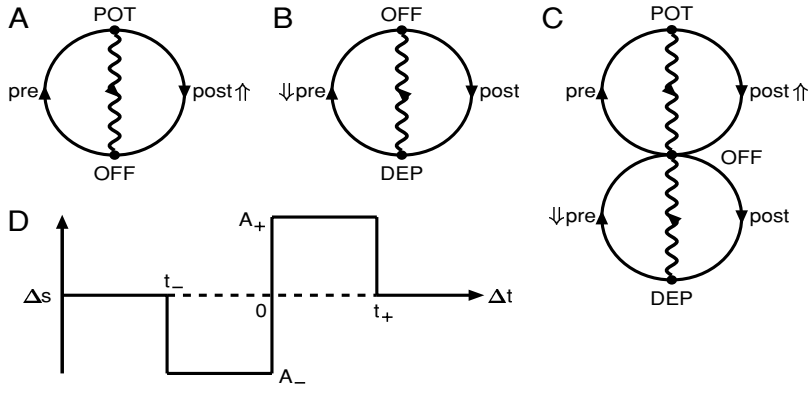

Figure 1: The simplest, self-consistent forms that the proposed synaptic switch can take, and its resulting plasticity rule. (A) The states and transitions that must exist in a switch accommodating the timing-dependent induction of LTP due to pre- and postsynaptic spiking. (B) Same as *A* but for the induction of LTD. (C) A unified three-state synaptic switch that can exhibit both LTP and LTD. (D) Change in synaptic strength evoked under the unified three-state switch for a representative spike pair at various spike timings. The arrows ⇑ and ⇓ indicate the induction of potentiation and depression, respectively.

The active transition $POT \rightarrow OFF$ is the only transition capable of inducing potentiation of synaptic strength.

To account for depression of synaptic strength under negatively correlated spiking, a second synaptic switch is postulated (see Figure 1B). This switch behaves in a similar manner to the one just described, except here, postsynaptic spiking triggers the initial active transition to a different functional state $OFF \rightarrow DEP$. When in the *DEP* state, further postsynaptic spiking has no effect, but a presynaptic spike will trigger the active transition $DEP \rightarrow OFF$ with an associated decrease in synaptic strength, by an amount A_-. The stochastic, passive transition $DEP \rightarrow OFF$ returns the switch to the *OFF* state in the absence of further spiking.

These two switch mechanisms adequately describe a step change in synaptic strength in response to positively or negatively correlated spiking. The two switches could exist independently, but we can unify them into a single, three-state synaptic switch (see Figure 1C). The parameters of this three-state switch are not necessarily symmetric, which in biological terms reflects the possible independence of the processes activated by pre- or postsynaptic firing when the synapse is in the *OFF* state. The modification induced by a representative spike pairing at various spike time differences is plotted in Figure 1D. The switch rule gives rise to a modification in accordance with a two-step function of fixed step heights, $A_\pm$. The two random step

widths, $t_{\pm}$, are governed by the probability distributions that describe the passive transitions $POT \to OFF$ and $DEP \to OFF$. If this hypothetical spike pairing were repeated, then the widths $t_{\pm}$ would likely take different values, giving rise to a different "critical window." It is important for our model that the magnitude of synaptic plasticity, represented by the heights of the two step functions, is not dependent on the difference in spike times. The level of coincidence detection required is therefore minimal, as the synapse is required only to record the occurrence of a pre- or postsynaptic spike, not the precise time of occurrence. Although additional states and transitions may freely be added, we find that this simple, self-consistent, three-state switch is all that is required to reproduce a variety of tLTP results.

We assume that an afferent makes multiple synapses onto a target cell. The overall strength of the connection between the two cells is defined, for simplicity and according to the usual convention, to be the linear sum of each individual synaptic strength. The synapses are treated independently, which, due to the stochastic nature of the synaptic modification rule, means that the synapses comprising a connection will often be in different states. It is therefore the spatial average over synapses, and the temporal average over spike pairs, that determines the overall change in connection strength.

3 Analysis of Model

For notational convenience, we denote a presynaptic spike by the symbol π and a postsynaptic spike by the symbol p. Pre- and postsynaptic firing are assumed to be independent Poisson processes with rates λ_π and λ_p, respectively, and we set $\beta = \lambda_\pi + \lambda_p$. Because they are independent, the combined pre- and postsynaptic spike sequences form a single Poisson process of overall rate β. For a Poisson process of rate λ, the inter-event time (the "waiting time") is an exponentially distributed random variable with parameter λ, and thus, in particular, the waiting time between any two spikes is exponentially distributed with parameter β and has the probability density function $f_T(t) = \beta e^{-\beta t}$. For any given spike in the combined train, the probability that it is presynaptic is λ_π/β, and the probability that it is postsynaptic is λ_p/β.

Here we restrict our analysis to spike trains consisting of two spikes only, so that a two-spike train can manifest itself as one of four possible sequences: $\pi\pi$, πp, $p\pi$, or pp. The probability of observing a particular spike pattern ij, where $i, j \in \{\pi, p\}$, is then just $p_{ij} = \lambda_i \lambda_j / \beta^2$. Longer spike trains are investigated numerically in section 4. Despite the more complicated nature of the higher-order interactions between multiple spikes, our results for longer spike trains share characteristics similar to those for the two-spike case.

Under a specific spike pattern, modification of synaptic strength may or may not occur, depending on the state of the switch when the second spike arrives. We therefore seek an expression for the expected change in synaptic efficacy induced by a single spike pair under our switch rule. The spike

patterns $\pi\pi$ and pp cannot cause a change in synaptic strength under our switch rule, so we need only to consider the πp and $p\pi$ patterns. Consider the πp pattern. The initial presynaptic spike triggers the active transition $OFF \to POT$. The switch remains in the POT state until either the arrival of the postsynaptic spike or the occurrence of a stochastic, passive transition. In either case, the switch will be returned to the OFF state, but the active transition triggered by the postsynaptic spike will also induce a change in synaptic strength. We therefore require the probability that the switch is still ON when the postsynaptic spike arrives. We assume that the probability density function $f_\Gamma(t)$ for the passive transition $POT \to OFF$ is given by a gamma probability density function of integer order n_+,

$$f_\Gamma(t) = \frac{(t/\tau_+)^{n_+-1}}{(n_+-1)!}\frac{1}{\tau_+}\exp(-t/\tau_+), \tag{3.1}$$

where τ_+ is the characteristic timescale associated with this switching process. As n_+ is an integer, this is equivalent to requiring the deactivation of n_+ independent exponential decay processes. These processes could, for example, represent the activation of n_+ independent signaling pathways in response to presynaptic spiking, all of which must deactivate for the switch to be considered OFF. The probability that the transition $POT \to OFF$ has occurred after a time t is then

$$P^+_{OFF}(t) = \int_0^t dt'\ f_\Gamma(t') = 1 - e^{-t/\tau_+}e_{n_+}(t/\tau_+), \tag{3.2}$$

where $e_n(t/\tau) = \sum_{i=0}^{n-1}(t/\tau)^i/i!$. The probability that the switch is ON after a time t is then $P^+_{ON}(t) = e^{-t/\tau_+}e_{n_+}(t/\tau_+)$. The mean change in synaptic efficacy triggered by the πp spike pair of time difference t is the amplitude of synaptic plasticity, A_+, multiplied by the chance that the switch is still ON at time t after the first spike, $P^+_{ON}(t)$. Thus, the conditional expectation value for the change in synaptic efficacy, $\Delta S_{\pi p}(t)$, given a πp spike time interval t, is just

$$\Delta S_{\pi p}(t) = +A_+ P^+_{ON}(t). \tag{3.3}$$

Similarly, an identical argument for the $p\pi$ sequence gives us

$$\Delta S_{p\pi}(t) = -A_- P^-_{ON}(t), \tag{3.4}$$

where P^-_{ON} is identical to P^+_{ON}, except that n_+ and τ_+ are replaced by n_- and τ_-, these being the parameters specifying the gamma distribution for the $DEP \to OFF$ stochastic transition. A representative plot of $\Delta S_{\pi p}(t) + \Delta S_{p\pi}(-t)$ as a function of spike time difference, t, is shown in Figure 2, with negative t corresponding to a $p\pi$ sequence and positive t corresponding

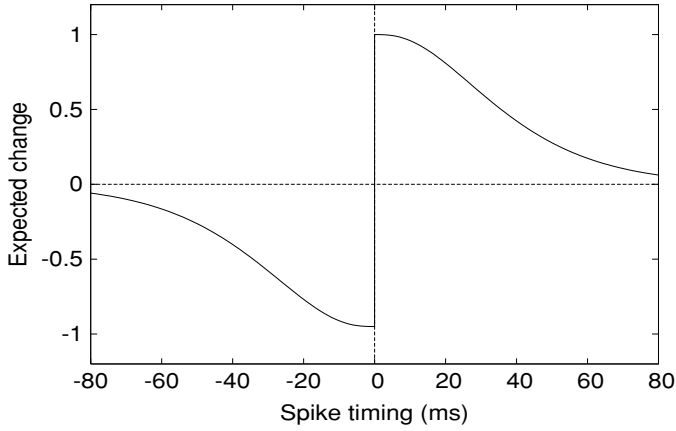

Figure 2: The expected change in synaptic strength as a function of the spike time difference t, from equations 3.3 and 3.4.

to πp sequence. Motivated by simplicity, and for approximate agreement with experimental data (Bi & Poo, 1998), we show the case where $A_+ = A_- = 1, n_+ = n_- = 3$ and $\tau_- = \tau_+ = 20$ ms. The form illustrated is relatively insensitive to the exact choice of parameters.

We may now obtain the unconditional expectation value for the synaptic modification arising from any pattern of two spikes, regardless of the spike time interval and the particular spike pattern. For the pattern ij, we weight its conditional expected synaptic change ΔS_{ij} by the probability of the pattern, p_{ij}, and we integrate out the spike times according to their probability density functions. The unconditional expection is given by the sum over all such patterns, so that

$$\mathbf{E}[\Delta S] = \sum_{i,j\in\{\pi,p\}} p_{ij} \int_0^\infty dt_1 \; f_T(t_1) \int_0^\infty dt_2 \; f_T(t_2) \Delta S_{ij}(t_2), \tag{3.5}$$

where, of course, $\Delta S_{\pi\pi}(t) = \Delta S_{pp}(t) = 0$. Defining

$$J_\pm(\lambda) = 1 - \frac{1}{(1+\lambda\tau_\pm)^{n_\pm}}, \tag{3.6}$$

we finally obtain

$$\mathbf{E}[\Delta S] = \frac{\lambda_\pi \lambda_p}{\beta^2} \left[A_+ J_+(\beta) - A_- J_-(\beta) \right] \tag{3.7}$$

as the expected synaptic change arising from any two-spike sequence.

This equation is an analytical expression for the expected change in synaptic efficacy induced by a two-spike train at given pre- and postsynaptic firing rates, λ_π and λ_p. In the limit of large λ_π and λ_p in equation 3.7, we have that $\mathbf{E}[\Delta S] \propto (A_+ - A_-)$. The sign of this expression indicates whether potentiation or depression of synaptic strengths is expected for high pre- and postsynaptic firing rates. Experimental work on rLTP shows that high pre- and postsynaptic firing rates generally lead to LTP (Sjöström, Turrigiano, & Nelson, 2001). This requires that $\mathbf{E}[\Delta S] > 0$ for large λ_π and λ_p, that is, $A_+ > A_-$. However, to be able to generate competitive dynamics, we also require a depressive phase where $\mathbf{E}[\Delta S] < 0$; otherwise, synapses can never weaken on average. Putting $\lambda_p = \lambda_\pi$, and maintaining the requirement that $A_+ > A_-$, a sufficient condition is that $\partial \mathbf{E}[\Delta S]/\partial \lambda_\pi|_{\lambda_\pi, \lambda_p = 0} < 0$. As $\mathbf{E}[\Delta S]|_{\lambda_\pi, \lambda_p = 0} = 0$, this guarantees the presence of a depressive region. This produces a second constraint,

$$\gamma = \frac{A_+ n_+ \tau_+}{A_- n_- \tau_-} < 1, \tag{3.8}$$

which we interpret as depression dominating over potentiation. An identical condition has been observed, but not mathematically derived, for simulations of exponential-like tLTP plasticity rules in the context of generating dynamics that give rise to bimodal synaptic distributions (Song et al., 2000). Empirical work has also shown it to be a requirement for a BCM-like learning rule to emerge on average from such rules (Izhikevich & Desai, 2003). Here, we have shown that requiring our switch rule to maintain, on average, a BCM-like learning rule leads to mathematically derivable constraints. Whether the presence of a depressive regime, for which $\gamma < 1$, guarantees the presence of competitive dynamics in our switch rule, is an issue that we shall explore elsewhere.

We set $A_+ = 1$ and $A_- = 0.95$, in accordance with the condition that $A_+ > A_-$, and choose $n_+ = n_- = 3$, as before. Setting $\tau_- = 20$ ms and choosing γ determines the remaining parameter τ_+. We also assume that the postsynaptic firing rate λ_p is linearly related to the presynaptic rate λ_π once it exceeds a value η, so that

$$\lambda_p = \begin{cases} \lambda_\pi - \eta & \text{for } \lambda_\pi \geq \eta \\ 0 & \text{for } \lambda_\pi < \eta \end{cases}, \tag{3.9}$$

and we set $\eta = 5$ Hz. Varying the presynaptic firing rate λ_π produces the family of curves shown in Figure 3 for different values of γ. When $\gamma < 1$, we observe that the behavior is qualitatively BCM-like, with a depressive phase at low presynaptic firing rates followed by a transition to potentiation as a threshold is passed. We find exact agreement, presented in section 4, between this analytical result and numerical simulation of two-spike trains.

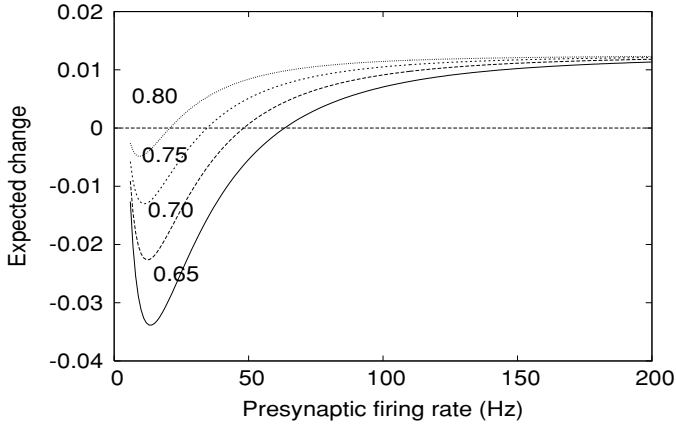

Figure 3: The expected change in synaptic strength due to a single pair of spikes, for values of γ shown attached to each curve. The pre- and postsynaptic cells fire according to a Poisson process.

For longer spike trains, equation 3.7 represents the expected change induced by any pair of spikes, not the expected change induced by all spike interactions in these processes. Nevertheless, for longer spike trains, the total change induced by multiple spike interactions is of a qualitatively similar character, as we will show in section 4. An important feature of the BCM model (Bienenstock et al., 1982) is the sliding of the potentiation threshold in response to changes in the postsynaptic firing rate (Kirkwood, Rioult, & Bear, 1996; Philpot, Espinosa, & Bear, 2003). As the analytical expression shows, a threshold emerges from our model that is a function of various, easily modifiable parameters. Allowing some of these parameters to depend on the recent time average of postsynaptic firing, in a manner similar to other modeling approaches, would capture the sliding threshold of the BCM rule in a satisfactory way.

4 Results

We now turn to numerical simulation to study the behavior of a single afferent innervating a single target cell. The connection between the afferent and target cells is assumed to comprise multiple synapses, which individually obey the stochastic switch rule set out above. The tLTP curve governing changes in overall connection strength emerges from the averaged effect of our synaptic switching rule. This averaging process can take place over multiple synapses or, equivalently, multiple spike pairings. We choose to simulate 10 synapses per afferent. This is partly so that an averaging process can be observed even with single spike pairs, but also to show that the synapses comprising a connection can often be in different states and

undergo different modifications while still giving rise to the tLTP curve when viewed as an ensemble. As the stimulation protocols used involve many spike pairings, the simulations can, in fact, be repeated with just one synapse. The averaging process then occurs at this one synapse over many events, and the results are qualitatively similar.

A typical tLTP or rLTP experimental protocol relies on evoking pre- and postsynaptic action potentials in synaptically coupled cells. In both cases, the normal function of a synapse as a propagator of neuronal activity is suppressed, with external current injections typically used to achieve spiking on demand. In our simulations, as in the experimental procedures, afferent and target cell spiking is assumed to be driven by an external force. Presynaptic spiking does not contribute to postsynaptic spiking in any way, and simulation of any kind of integrate-and-fire target cell is not required.

Due to a high level of variability, the majority of experimental data on tLTP describes relative changes in connection strength. Multiple spike pairings are needed to evoke a statistically significant change in overall connection strength. We adopt a similar approach by defining the combined initial synaptic strength of the input afferent to be equal to 1, and then scaling the magnitudes of synaptic plasticity, A_+ and A_-, to reproduce the measured relative change in overall connection strength under a particular experimental protocol.

4.1 Spike-Based Results. In order to examine the timing dependence of our rule, we implement a particular experimental protocol that has been shown to evoke tLTP-like changes in embryonic rat hippocampal cultures (Bi & Poo, 1998). This protocol is typical of timing-based LTP experiments, and our parameters are chosen to reflect the main features of these data. As described above, we set $n_+ = n_- = 3$, $A_+ = 1.00$, $A_- = 0.95$, and $\tau_- = 20$ ms. Choosing $\gamma = 0.70$ generates a value for $\tau_+ = \gamma A_- \tau_- / A_+ \simeq 13$ ms. The magnitudes of synaptic plasticity, A_+ and A_-, set the overall scale for synaptic modifications. To match the experimental data, we require that the maximum possible relative change in overall connection strength evoked by 60 spike pairings is approximately ± 1. We therefore require a scaling factor of 60 to be applied to the magnitudes of synaptic modification, and we set $A_+ = 1.00/60$ and $A_- = 0.95/60$ accordingly. This scaling has no other effect beyond producing a simulated change in overall connection strength equal to the experimentally observed value, and the dynamics of the synaptic switch are unchanged. Noise in the timing of spikes, reflecting both experimental error and variable transmission times, is drawn from a gaussian distribution with standard deviation of 1 ms. The spike pairing protocol consists of 60 pairings at 1 Hz applied at time differences ranging from -80 ms to $+80$ ms (Bi & Poo, 1998). The averaging of the synaptic modification rule over multiple synapses and pairings gives an overall change in connection strength that has two exponential-like phases, plotted in Figure 4. This change is consistent with experimental data (Bi & Poo, 1998), with polarity

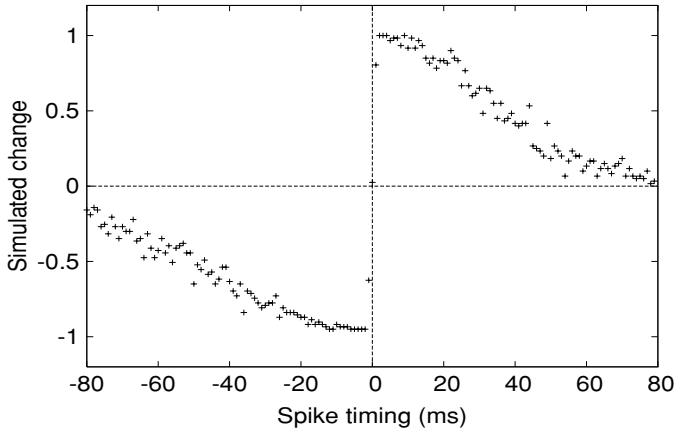

Figure 4: Simulated total change in overall connection strength as spike timing varies.

depending only on the signs of $A_{\pm}$. These simulation results agree with the analytical expressions and are qualitatively unchanged for any realistic level of temporal gaussian noise with a standard deviation $\sigma \leq 10$ ms. The parameters $\tau_{\pm}$ determine the width of the temporal window—as $\tau_{\pm}$ increase, spike pairings at greater time differences begin to evoke a significant change in synaptic efficacy. As discussed above, $A_{\pm}$ determine the maximum amplitude of plasticity, evoked when the time difference is very small. Adjustment of these parameters produces a family of tLTP curves that can reproduce a variety of experimental results without altering the basic characteristics, such as the exponential-like slopes, of the curve.

A number of more complicated spike patterns, including triplets and quadruplets, have been explored in experimental preparations (Froemke & Dan, 2002). In the case of spike triplets, the experimental protocols are very similar to that of spike pairings, but instead of one pre- and one postsynaptic spike, an additional third spike (either pre- or postsynaptic) is introduced. We reproduce the experimental protocol exactly, repeating a particular stimulation pattern 60 times at 0.2 Hz. The parameters are the same as for the spike pairing simulations, and the results are set out in Table 1. The simulated results for the spike-triplet protocols are in close agreement with experiment (Froemke & Dan, 2002), a result that cannot be reproduced under other modification rules without additional constraints on spike interaction such as spike suppression (Froemke & Dan, 2002). Under earlier models of tLTP, spike triplets were treated as two separate spike pairings that individually obeyed a tLTP-like modification curve. Their linear addition gives a predicted change that is not in agreement with experimental data. Here, the switch provides a mechanism, in the form of the passive transitions to the

Table 1: Experimental and Simulated Effect of Spike Triplets and Quadruplet.

Pattern	Timing (ms)	Experiment	Simulation
$\pi p \pi$	2.6/6.0	$\uparrow$	+1.00
$p \pi p$	6.5/0.5	$\downarrow$	−0.94
$\pi p p \pi$	8.8/10.6/9.6	$\uparrow$	+0.03
$p \pi \pi p$	7.9/9.6/9.0	$\downarrow$	+0.03

Notes: The first column gives the spiking patterns (a presynaptic spike is denoted by π and a postsynaptic spike by p). The second column gives the spike time differences for the patterns. The third column gives an indication of the experimental measurement (Froemke & Dan, 2002); upward arrows indicate potentiation, and downward arrows indicate depression. The fourth column gives our simulated results.

OFF state, under which a triplet can evoke a change with a sign opposite to that predicted by such linear addition of pairings respecting the tLTP curve. With two presynaptic spikes and one postsynaptic spike, the first presynaptic spike moves the switch into the *POT* state. If the postsynaptic event occurs in a timely fashion, it will move the switch back to the *OFF* state and trigger an increase in synaptic strength. In this case, the second presynaptic event will move the switch to only the *POT* state, and this does not trigger any change in synaptic strength. If, however, the postsynaptic event occurs too late and the switch has already returned to the *OFF* state via a passive transition, then the switch will instead be moved to the *DEP* state. In this case, the second presynaptic event moves the switch back to *OFF* and triggers a depression of synaptic efficacy. It is the choice of parameters describing the switch, $A_{\pm}$, $n_{\pm}$, and $\tau_{\pm}$, that determines the average outcome for a given protocol. In fact, the parameters chosen roughly to reflect simple spike pairing results are sufficient to accommodate spike triplets. This explanation of triplet interactions emerges as a natural consequence of the switch rule, with no need for modifications or additional constraints.

In the case of spike quadruplets, comprising of two pre- and two postsynaptic spikes, the switch rule leads to potentiation under both of the protocols set out in Table 1. This is not in agreement with the experimental results, where the second quadruplet protocol leads to depression. It is possible to accommodate the quadruplet results, leaving the pair and triplet results unchanged, by replacing the active transitions $POT \rightarrow OFF$ and $DEP \rightarrow OFF$ with active $POT \rightarrow POT$ and $DEP \rightarrow DEP$ transitions, respectively. However, such a modification of our switch rule destroys the stability of the rate-based limit (unpublished results), and this seems to be a high price to pay to account for results whose significance is currently unclear.

4.2 Rate-Based Results. Induction of LTP using a rate-based protocol was simulated by driving the presynaptic cell at a fixed frequency (ranging

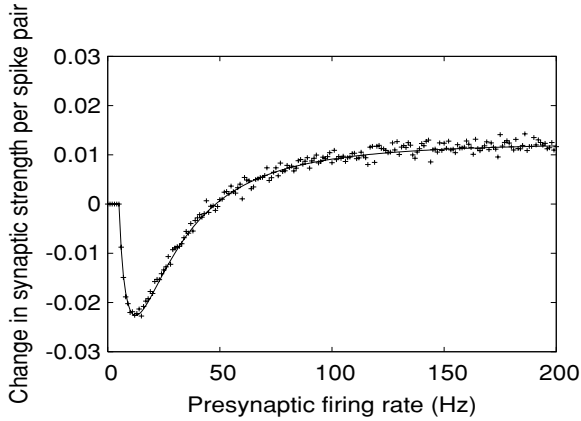

Figure 5: Change in overall connection strength, per pair of spikes, for simulated two-spike trains, as a function of presynaptic firing rate. The solid line shows the corresponding analytical result.

from 0–200 Hz) governed by a Poisson process, as set out above. The postsynaptic cell fires in a similar, Poisson manner, with frequency given by equation 3.9. This suppresses postsynaptic firing at very low presynaptic rates, as would be expected in a real system with many inputs. The cells are decoupled in the sense that presynaptic firing does not influence the postsynaptic cell membrane potential in any way, thus reproducing a typical experimental protocol in which two cells are held in current clamps and current injections are used to induce spiking (Bi & Poo, 1998). The parameters are identical to the spike-pairing simulations. In order to verify our analytical results, we first simulate the effect of pairs of spikes by truncating the simulation after the first pair of events. Each pair of events can therefore consist of two presynaptic spikes, two postsynaptic spikes, or one of each. The average, overall connection change after a total of 10^6 total spikes is shown in Figure 5, as a function of the presynaptic firing rate. We see exact agreement between the simulated two-spike interaction and the analytically derived result, equation 3.7.

The two-spike results consider spike trains containing exactly two events, the interactions of which give rise to a BCM-like change in the overall connection strength. An identical change will arise from the interaction of any pair of spikes in a train provided that the synapse is in the *OFF* state. However, when longer pre- and postsynaptic spike trains are considered, further spike interactions may occur, and it is important to show that the qualitative form of the two-spike learning rule is unchanged by these higher-order corrections. We therefore simulate longer spike trains, of 50 and 100 spikes. The total change in overall connection strength then arises from a summation

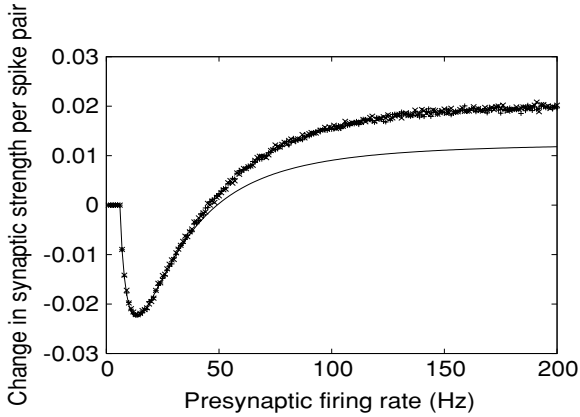

Figure 6: Change in overall connection strength, per pair of spikes, for simulated trains of 50 spikes (vertical crosses) and 100 spikes (diagonal crosses), as a function of presynaptic firing rate. The change per pair of spikes for a 50-spike train is almost identical to that for the 100-spike train. Also shown for comparison is the analytical two-spike result, represented by the solid line.

of the many individual transitions that occur. The simulated overall connection change per spike pair, averaged over many such trains, is shown in Figure 6, allowing a direct comparison to the two-spike train result, which is also shown. An averaged, BCM-like plasticity rule emerges in all cases. The 50- and 100-spike trains give an average change per spike pair that is different from that calculated for simple two-spike trains, reflecting the influence of higher-order interactions between the spikes, but the results are nevertheless qualitatively similar. The higher-order interactions are of smaller and smaller significance, with the average change in connection strength per pair of spikes converging to a limiting value as the number of spikes in a train grows large. Thus, as intuitively expected, if we were to plot the total change after the 100-spike train, it would simply be twice the total change after the 50-spike train.

5 Discussion

Spike-timing-dependent plasticity has received considerable attention in recent years. From a modeling perspective, two broad approaches to this novel form of synaptic plasticity have been adopted. The first approach assumes that the observed tLTP curves are an accurate description of the synaptic plasticity rule operating at each individual synapse between an afferent and its target (Song et al., 2000; van Rossum et al., 2000). The computational consequences of such an assumption are then determined. The second approach does not take the rules over directly, but rather attempts

to derive them from a more detailed, biophysically plausible analysis of the molecular machinery present in synapses (Castellani et al., 2001; Karmarkar & Buonomano, 2002; Shouval et al., 2002). Although the second approach promises a deeper and more general understanding, models of this type are commonly beset by a variety of problems, including sensitivity to parameter choices and the prediction of an extra depression window for large spike time differences. Common to both approaches is the view that tLTP must be valid, at some level, at individual synapses for a single spike pair. Hence, individual synapses in such models are required to represent in some form the spike timing difference and adjust their strengths accordingly.

In contrast, we consider that the experimental data for tLTP cannot be divorced from the experimental protocols used to obtain them. Rarely are monosynaptically coupled pairs of neurons studied, so that the changes in synaptic efficacy that are observed are mostly the results of the many changes in the strengths of the individual synapses that constitute the overall synaptic connection between afferent and target. Furthermore, the data are always obtained from a protocol in which multiple spike pairings are employed (Bi & Poo, 1998). Although it is entirely possible that the observed tLTP curves are, in fact, respected by individual synapses during a single spike pairing, so that the experimental averaging procedure over both multiple synapses and multiple spike pairings does faithfully report the underlying plasticity rule, we have instead sought to determine whether the observed tLTP rule can, in fact, arise from the synaptic and temporal average of individual synaptic changes respecting a much simpler plasticity rule.

In this letter, we have indeed shown that such an alternative view is viable. The resulting model is susceptible to some degree of understanding and analysis, and very much reduces the computational demands placed on synapses. We have postulated that an individual synapse, when presented with a pre- and postsynaptic spike pair, adjusts its synaptic strength by a constant positive or negative jump or does not change its strength at all. Our hypothetical synapse is therefore required only to record the occurrence of a pre- or postsynaptic event and adjust its strength by a fixed amount if an appropriate spike is generated in a timely fashion. Provided that the synapse destroys this record in some stochastic manner, so that the trace is short-lived, we have shown that we can derive the tLTP rule directly. Thus, a simple synaptic modification rule can indeed give rise directly to a much more complex tLTP rule. The tLTP rule can thus be viewed as an average, ensemble, emergent property of neurons, where the average is over either multiple synapses or multiple spike pairings (or both). Such a view is analogous, for example, to the relationship between thermodynamics and statistical mechanics in physics. The gas laws, such as Boyle's law, are not followed by individual gas molecules, but rather emerge, statistically, from the underlying motions of molecules following Newton's laws. Temperature and pressure are not intrinsic properties of individual gas molecules,

but emerge as properties of the collective system. Just so, we propose that tLTP is not an intrinsic property of individual synapses, but emerges as an ensemble property when much simpler rules are averaged over many synapses and over many spike pairs.

Our switch rule also provides a mechanism by which spike triplets may naturally give rise to an overall change in connection strength similar to that observed in experiment. Under typical tLTP models (Song et al., 2000) this result can be achieved by introducing additional nonlinearities, such as spike suppression (Froemke & Dan, 2002). In our model, once a synapse is in, say, the *POT* state, this state cannot be changed by further presynaptic spikes until the synapse returns to the *OFF* state. In a strict sense, the synapse suppresses the effect of these subsequent presynaptic spikes, but this nonlinearity is of a rather different form from that proposed by Froemke and Dan (2002), in which the values of A_+ and A_- are scaled depending on the spike history.

A biophysical implementation of a simple tTLP rule based around NMDA receptor dynamics has also been proposed (Senn, Markram, & Tsodyks, 2001). It is hypothesized that a fixed population of NMDA receptors undergoes transitions between three different functional states dependent on pre- and postsynaptic spiking. Spike times are encoded by allowing activated NMDA receptors individually to decay back to the unactivated state. The proportion of the population of the NMDA receptors remaining in the activated state determines the adjustment to the synaptic strength in a graded, continous manner. Such a model can reproduce a variety of tLTP results. Under our switch rule, we propose a superficially similar three-state switch mechanism, but it is the entire synapse that enters different functional states rather than individual NMDA receptors. Moreover, the synapse adjusts its strength in a fixed, all-or-none manner. The observed tLTP rule in our model is therefore an emergent property of the whole set of synapses, with single synapses obeying a much simpler rule.

We have deliberately presented our switch rule in the simplest form possible that is consistent with a variety of spike-timing data. This permits a degree of analytical understanding of the rule, enabling us to determine the properties of the model without resorting to a purely numerical approach. Although our switch rule does indeed accommodate a wide range of experimental results, it is unrealistic to expect our model to be comprehensive at this stage. We note, in particular, that the frequency dependence of the tLTP observed in neocortical pyramidal cells (Markram & Tsodyks, 1996) is not captured by our model in its present form. We will explore this, and similar issues, in future work.

Here we have referred to spatial (and temporal) averaging and have used standard probability theory to calculate, in an exact rather than approximate manner, the average change in synaptic efficacy either over time or over a large number of synapses, where the averaging arises due to the probabilitistic nature of our proposed switch mechanism and the intrinsic

stochasticity of Poisson spike trains. In mean field approaches (Kistler & van Hemmen, 2000; Gerstner, 2001; Kempter, Leibold, Wagner, & van Hemmen, 2001; Senn, 2002), quantities are replaced by their local spatial averages so that the resulting approximate equations are more analytically tractable. However, the averaging in our model is exact and real, in the sense that we are proposing that real experiments actually measure these average, emergent properties of neurons.

We have also shown that a BCM-like rate-based rule (rather than spike-based rule) can be formally derived from our model. This derivation requires no further assumptions and produces two explicit constraints on the choice of parameters. First, in order to generate LTP when both pre- and postsynaptic firing rates are high, we require that $A_+ > A_-$. That is, the level of potentiation induced under our switch rule by a presynaptic spike followed by a postsynaptic spike must be greater than the level of depression induced when the spike order is reversed. Second, in order to generate LTD at low firing rates, we require that $\gamma = (A_+ n_+ \tau_+)/(A_- n_- \tau_-) < 1$. This may be interpreted as depression dominating over potentiation. An identical condition has been observed to be a requirement for generating bimodal synaptic distributions under a simple, additive tLTP rule (Song et al., 2000) and in other models too (Gerstner, 2001; Kempter et al., 2001). The conditions for the derivation of BCM-like rules from tLTP rules have also been studied (Senn et al., 2001; Izhikevich & Desai, 2003; Burkitt, Meffin, & Grayden, 2004), it being found that by restricting spike interactions, BCM-like rules may be derived from a variety of tLTP models.

Again, BCM implementations have usually been considered at the level of individual synapses, with the synapse required to perform complex computations, possibly represented at some abstract level, to determine the magnitude and direction of change of synaptic strength. However, the BCM-like rule we see arising from our switch rule is an emergent property that does not place such burdens on each synapse. In fact, the BCM-like rule in our model is "doubly" emergent, requiring first the emergence of the tLTP rule. Mathematically, this tLTP rule takes the form of a conditional expectation value for synaptic change, conditional, that is, on a given spike time difference. Second, to turn this conditional expectation value into an unconditional value, we must weight it by some probability density function for the spike time difference and the probabilities of each possible spike pair. Thus, in order to obtain the BCM-like rule, we assumed that the spike time difference distribution originated from Poisson spike trains. Had we chosen to drive the afferents in some other, non-Poisson manner, a different rate-based synaptic plasticity rule may have emerged. In this sense, the BCM rule emerges from an interaction between the tLTP rule, which is itself emergent, and how we have decided to drive the afferents. This suggests the possibility that apparently different rate-based rules may in fact merely reflect different choices available to the experimenter in how he decides to probe his experimental system, or indeed that as synaptic patterns change and hence

neuronal firing patterns change, the nervous system may slowly change its own rate-based learning rule. We shall pursue this idea in future work.

The most direct test of our synaptic switch hypothesis would be to observe the change in efficacy at an individual synapse induced by a pre- and postsynaptic spike pair. We predict that the changes in synaptic efficacy would be seen to occur in jumps of fixed magnitude, not as a smoothly varying function of the pre- and postsynaptic spike timing difference. Such a result would provide strong evidence that the observed tLTP window is not instantiated at the level of individual synapses and support our hypothesis that the window emerges only as an ensemble property of neurons. Indeed, in measuring LTP at putatively monosynaptically coupled pairs of hippocampal neurons, Peterson, Malenka, Nicoll, and Hopfield (1998) found all-or-none potentiation rather than a continuous change, possibly consistent with our approach. Such "binary" synapses have also been studied in other contexts and have been shown to reproduce various tLTP results (Fusi, Annunziato, Badoni, Salamon, & Amit, 2000; Fusi, 2002).

We have proposed that single synapses implement something akin to a three-state switch, and from this have derived a tLTP rule and a BCM-like rule. Where might the machinery that implements this switch reside? The switch moves from the *OFF* state to the *DEP* state following a postsynaptic spike. All of a target's input synapses might thus be expected to move into the *DEP* state, and this suggests that the natural locus for the *DEP* state of the switch may be the postsynaptic aspect of the synapse. An active transition back to the *OFF* state caused by a presynaptic spike may then cause a postsynaptic change in the synapse, resulting, for example, in the removal of some neurotransmitter receptors from the postsynaptic membrane, leading to a decrease in synaptic strength. Similarly, when the switch moves from the *OFF* state into the *POT* state following a presynaptic spike, all of the afferent's output synapses might be expected to move into the *POT* state, and so this perhaps suggests a presynaptic locus for the *POT* state of the switch. An active transition to the *OFF* state caused by a postsynaptic spike may, this time, change the presynaptic aspect of the synapse, perhaps enhancing neurotransmitter release or even inducing terminal synaptic sprouting, so that synaptic strength is increased. Thus, the switch may actually be distributed across the entire synapse rather than confined exclusively to the pre- or postsynaptic side of the synapse. However, given the ubiquity of both anterograde and retrograde messengers in the nervous system, we should be cautious in using such arguments: the mathematical details of the switch do not commit us to any particular view concerning its exact locus or to the precise molecular machinery involved in its implementation. Regarding this latter issue of molecular implementation, we can certainly imagine many different scenarios and appeal to many different candidate molecules known to be involved in synaptic plasticity. Indeed, it is entirely possible that while the switch may be implemented broadly across the nervous system, the machinery implementing it may also vary broadly from system to

system. To this extent, our proposal for a synaptic plasticity switch, within the framework of which we have shown that a broad range of experimental results on synaptic plasticity can be understood, does not stand or fall or any given mechanism, but to some extent stands above although is consistent with many different possible implementation details.

Acknowledgments

P.A.A. thanks the University of Southampton for the support of a studentship. T.E. thanks the Royal Society for the support of a University Research Fellowship.

References

Bell, C. C., Han, V. Z., Sugawara, Y., & Grant, K. (1997). Synaptic plasticity in a cerebellum-like structure depends on temporal order. *Nature*, *387*, 278–281.

Bi, G. Q., & Poo, M. M. (1998). Synaptic modifications in cultured hippocampal neurons: Dependence on spike timing, synaptic strength, and postsynaptic cell type. *J. Neurosci.*, *18*, 10464–10472.

Bienenstock, E. L., Cooper, L. N., & Munro, P. W. (1982). Theory for the development of neuron selectivity: Orientation specificity and binocular interaction in visual cortex. *J. Neurosci.*, *2*, 32–48.

Bliss, T. V. T., & Lømo, T. (1973). Long-lasting potentiation of synaptic transmission in the dentate area of the anaesthetized rabbit following stimulation of the perforant path. *J. Physiol.*, *232*, 331–356.

Burkitt, A. N., Meffin, H., & Grayden, D. B. (2004). Spike-timing-dependent plasticity: The relationship to rate-based learning for models with weight dynamics determined by a stable fixed point. *Neural Comput.*, *16*, 885–940.

Castellani, G. C., Quinlan, E. M., Cooper, L. N., & Shouval, H. Z. (2001). A biophysical model of bidirectional synaptic plasticity: Dependence on AMPA and NMDA receptors. *Proc. Natl. Acad. Sci. USA*, *98*, 12772–12777.

Debanne, D., Gähwiler, B. H., & Thompson, S. M. (1998). Long-term synaptic plasticity between pairs of individual CA3 pyramidal cells in rat hippocampal slice culture. *J. Physiol.*, *507*, 237–247.

Dudek, S. M., & Bear, M. F. (1992). Homosynaptic long-term depression in area CA1 of hippocampus and effects of N-methyl-D-aspartate receptor blockade. *Proc. Natl. Acad. Sci. USA*, *89*, 4363–4367.

Egger, V., Feldmeyer, D., & Sakmann, B. (1999). Coincidence detection and changes of synaptic efficacy in spiny stellate neurons in rat barrel cortex. *Nat. Neurosci.*, *2*, 1098–1105.

Feldman, D. E. (2000). Timing-based LTP and LTD at vertical inputs to layer II/III pyramidal cells in rat barrel cortex. *Neuron*, *27*, 45–56.

Froemke, R. C., & Dan, Y. (2002). Spike-timing-dependent synaptic modification induced by natural spike trains. *Nature*, *416*, 433–438.

Fusi, S. (2002). Hebbian spike-driven synaptic plasticity for learning patterns of mean firing rates. *Biol. Cybern.*, *87*, 459–470.

Fusi, S., Annunziato, M., Badoni, D., Salamon, A., & Amit, D. J. (2000). Spike-driven synaptic plasticity: Theory, simulation, VLSI implementation. *Neural Comput.*, *12*, 2227–2258.

Gerstner, W. (2001). Coding properties of spiking neurons: Reverse and cross-correlations. *Neural Networks*, *14*, 599–610.

Gustafsson, B., Wigström, H., Abraham, W. C., & Huang, Y.-Y. (1987). Long-term potentiation in the hippocampus using depolarizing current pulses as the conditioning stimulus to single volley synaptic potentials. *J. Neurosci.*, *7*, 774–780.

Izhikevich, E. M., & Desai, N. S. (2003). Relating STDP to BCM. *Neural Comput.*, *15*, 1511–1523.

Karmarkar, U. R., & Buonomano, D. V. (2002). A model of spike-timing dependent plasticity: One or two coincidence detectors? *J. Neurophysiol.*, *88*, 507–513.

Kempter, R., Leibold, C., Wagner, H., & van Hemmen, L. J. (2001). Formation of temporal-feature maps by axonal propagation of synaptic learning. *Proc. Natl. Acad. Sci. USA*, *98*, 4166–4171.

Kirkwood, A., Rioult, M., & Bear, M. F. (1996). Experience-dependent modification of synaptic plasticity in visual cortex. *Nature*, *381*, 526–528.

Kistler, W. M., & van Hemmen, L. J. (2000). Modeling synaptic plasticity in conjunction with the timing of pre- and postsynptic action potentials. *Neural Comput.*, *12*, 385–405.

Markram, H., Lübke, J., Frotscher, M., & Sakmann, B. (1997). Regulation of synaptic efficacy by coincidence of postsynaptic APs and EPSPs. *Science*, *275*, 213–215.

Markram, H., & Tsodyks, M. (1996). Redistribution of synaptic efficacy between neocortical pyramidal neurons. *Nature*, *382*, 807–810.

Nishiyama, M., Hong, K., Mikoshiba, K., Poo, M. M., & Kato, K. (2000). Calcium stores regulate the polarity and input specificity of synaptic modfication. *Nature*, *408*, 584–588.

Peterson, C. C. H., Malenka, R. C., Nicoll, R. A., & Hopfield, J. J. (1998). All-or-none potentiation at CA3-CA1 synapses. *Proc. Natl. Acad. Sci. USA*, *95*, 4732–4737.

Philpot, B. D., Espinosa, J. S., & Bear, M. F. (2003). Evidence for altered NMDA receptor function as a basis for metaplasticity in the visual cortex. *J. Neurosci.*, *23*, 5583–5588.

Roberts, P. D., & Bell, C. C. (2002). Spike timing dependent synaptic plasticity in biological systems. *Biol. Cybern.*, *87*, 392–403.

Senn, W. (2002). Beyond spike timing: The role of nonlinear plasticity and unreliable synapses. *Biol. Cybern.*, *87*, 344–355.

Senn, W., Markram, H., & Tsodyks, M. (2001). An algorithm for modifying neurotransmitter release probability based on pre- and postsynaptic spike timing. *Neural Comput.*, *13*, 35–67.

Shouval, H. Z., Bear, M. F., & Cooper, L. N. (2002). A unified model of NMDA receptor-dependent bidirectional synaptic plasticity. *Proc. Natl. Acad. Sci. USA*, *99*, 10831–10836.

Sjöström, P. J., Turrigiano, G. G., & Nelson, S. B. (2001). Rate, timing and cooperativity jointly determine cortical synaptic plasticity. *Neuron*, *32*, 1149–1164.

Song, S., Miller, K., & Abbott, L. F. (2000). Competitive Hebbian learning through spike-timing-dependent synaptic plasticity. *Nat. Neurosci.*, *3*, 919–926.

van Rossum, M. C. W., Bi, G. Q., & Turrigiano, G. G. (2000). Stable Hebbian learning from spike-timing-dependent plasticity. *J. Neurosci.*, *20*, 8812–8821.

Zhang, L. I., Tao, H. W., Holt, C. E., Harris, W. A., & Poo, M. M. (1998). A critical window for cooperation and competition among developing retinotectal synapses. *Nature*, *395*, 37–44.

Received July 8, 2004; accepted March 29, 2005.